



Hot deformation behavior and processing map of Cu–Ni–Si–P alloy

Yi ZHANG¹, Ping LIU², Bao-hong TIAN¹, Yong LIU¹, Rui-qin LI¹, Qian-qian XU¹

1. College of Materials Science and Engineering,
Henan University of Science and Technology, Luoyang 471003, China;

2. College of Materials Science and Engineering,
University of Shanghai for Science and Technology, Shanghai 200093, China

Received 3 July 2012; accepted 10 March 2013

Abstract: The high-temperature deformation behavior of Cu–Ni–Si–P alloy was investigated by using the hot compression test in the temperature range of 600–800 °C and strain rate of 0.01–5 s^{−1}. The hot deformation activation energy, Q , was calculated and the hot compression constitutive equation was established. The processing maps of the alloy were constructed based on the experiment data and the forging process parameters were then optimized based on the generated maps for forging process determination. The flow behavior and the microstructural mechanism of the alloy were studied. The flow stress of the Cu–Ni–Si–P alloy increases with increasing strain rate and decreasing deformation temperature, and the dynamic recrystallization temperature of alloy is around 700 °C. The hot deformation activation energy for dynamic recrystallization is determined as 485.6 kJ/mol. The processing maps for the alloy obtained at strains of 0.3 and 0.5 were used to predict the instability regimes occurring at the strain rate more than 1 s^{−1} and low temperature (≤650 °C). The optimum range for the alloy hot deformation processing in the safe domain obtained from the processing map is 750–800 °C at the strain rate of 0.01–0.1 s^{−1}. The characteristic microstructures predicted from the processing map agree well with the results of microstructural observations.

Key words: Cu–Ni–Si–P alloy; hot compression deformation; dynamic recrystallization; constitutive equation; processing maps

1 Introduction

The integrated circuit is an important component of lead frame material and foundation of electronic information industry. Copper base alloys are used for electrical parts such as electrical connectors and lead frames because of their high electrical conductivity. The most commonly used alloys for the industrial application are based on the Cu–Be system, but they have the limitation of toxicity and high cost of production. Therefore, attempt have been made to develop other alloys having similar mechanical and physical properties. Cu–Ni–Si alloys possess good thermal and electrical conductivity and relatively higher strength, so they have attracted considerable interest in their application to integrated circuit lead frame [1–5].

Recently, a number of studies have been carried out on the hot deformation of Cu–Ni–Si alloys using hot compression test. ZHANG et al [6] studied the flow

behavior of Cu–8.0Ni–1.8Si–0.15Mg alloy within the temperature range of 600–950 °C. They suggested a hyperbolic sine equation to predict the flow stress of the alloys. In another research work, NIEWCZAS et al [7] investigated the hot compression behavior of Cu–Ni–Si–Cr–Mg alloy. The strain-induced localized Ni₂Si precipitate and intensive coarsening of precipitates at grain boundaries during hot deformation of Cu–Ni–Si–Cr–Mg alloy were found to be dominating reasons for flow softening.

In this work, the hot compression tests of Cu–Ni–Si–P alloy were carried out at the temperatures of 600–800 °C and strain rate ranging from 0.01 to 5 s^{−1} up to 60% height reduction. The effects of the deformation conditions on the flow behavior and microstructural evolution of Cu–Ni–Si–P alloy during compression deformation at elevated temperature were studied. The hot deformation activation energy, Q , was calculated and hot compression constitutive equation was established. The processing maps at different strains were established.

2 Experimental

The experiments were carried out on Cu–Ni–Si–P alloy with main chemical compositions 2.0%Ni, 0.5%Si, 0.03%P and Cu balance (mass fraction). The alloy was prepared in a 10 kg intermediate frequency induction furnace at the pouring temperature of 1300–1350 °C. The cylindrical specimens with 10 mm in diameter and 15 mm in height were machined from the forged rods which were solution treated at 900 °C for 1 h. Figure 1 presents the microstructure of Cu–Ni–Si–P alloy after solution treatment at 900 °C for 1 h. The flat ends of the specimen were recessed to a depth of 0.2 mm to entrap the lubricant of graphite mixed with machine oil during hot deformation so that the friction at the specimen/die surface could be minimized. The isothermal compression tests were conducted on a Gleeble–1500D simulator at the deformation temperature from 600 to 800 °C and the strain rate from 0.01 to 5 s^{−1}. All the specimens were heated with a heating rate of 10 °C/s and soaked for 180 s at the deformation temperature before isothermal compression. The deformation temperature was controlled in the accuracy of ±2 °C. The specimens were deformed to the height reductions of 60%, and then cooled down by water spraying to room temperature. Temperature of the specimen was monitored with the aid of a chromel/alumel thermocouple embedded in a 0.5 mm hole drilled half the height of the specimen. After compression testing, the specimens were immediately quenched in water. The deformed specimens were sectioned parallel to the compression axis and the microstructure examination was conducted by an OLYMPUS-PM3 optical microscope.

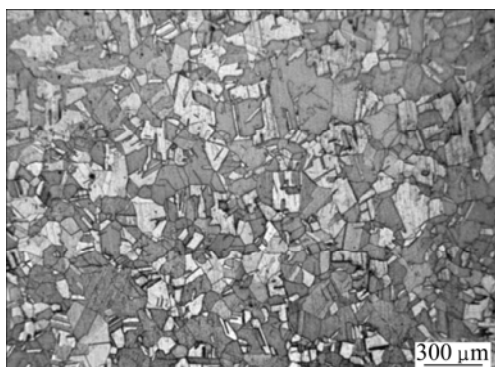


Fig. 1 SEM image of Cu–Ni–Si–P alloy after solution treatment at 900 °C for 1 h

3 Results and discussion

3.1 Flow stress behavior

The stress—strain curves at different deformation

temperatures are shown in Fig. 2. The flow stress decreases greatly with the increase of temperature at the same strain rate, while the true stress increases greatly with the increase of strain rate at the same temperature. The flow stress obtained at high temperature (750–800 °C) increases to a maximum value at first and then decreases until attains a steady state. Such behaviors have been shown to be typical for dynamic recrystallization taking place under hot deformation. The higher the deformation temperature is, the faster the dynamic recrystallization starts. However, at temperatures below 650 °C the flow stress keeps increasing to high strains and no indication of dynamic recrystallization can be seen. In this temperature range, the work hardening plays a main role in the plastic deformation of alloy. From the aforementioned stress—strain character, the results indicate that the work hardening effect is pronounced at higher strain rate and lower temperature. For the higher temperature and lower strain rate, the stress—strain curves show transient flow softening behaviour. With the increase of temperature, the second phase gradually grows up, so the alloy is prone to soften with high temperature compression. Therefore, it can be roughly concluded that the dynamic recrystallization temperature of alloy is around 700 °C and the analysis of flow stress variation can prove it. The actual softening mechanisms will be discussed in detail in the following section by comparison analysis with hot deformation activation energy calculations, processing maps and microstructural observation.

3.2 Constitutive equation

Arrhenius equation is widely used to describe the relationship between the strain rate, the flow stress and temperature at high temperatures [8–13]. The equation can be written as

$$\dot{\varepsilon} = A[\sinh(\alpha\sigma_p)]^n \exp[-Q/(RT)] \quad (1)$$

where $\dot{\varepsilon}$ is the strain rate; T is the thermodynamic temperature; σ_p is generally taken as the peak stress; R is the gas constant; Q is the activation energy for hot deformation; A , n and a are material constants.

To simplify the equation, we get the natural logarithms of both sides of Eq. (1):

$$\ln \sinh(\alpha\sigma_p) = -\frac{1}{n} \ln A + \frac{1}{n} \ln \dot{\varepsilon} + \frac{1}{n} \cdot \frac{Q}{RT} \quad (2)$$

Q can be expressed as

$$Q = R \frac{\partial \ln[\sinh(\alpha\sigma)]}{\partial (1/T)} \bigg|_{\dot{\varepsilon}} \frac{\partial \ln \dot{\varepsilon}}{\partial \ln[\sinh(\alpha\sigma)]} \bigg|_T \quad (3)$$

Figures 3(a) and (b) show the relationships between $\ln \dot{\varepsilon}$ and $\ln \sigma$, and between $\ln \dot{\varepsilon}$ and σ . The

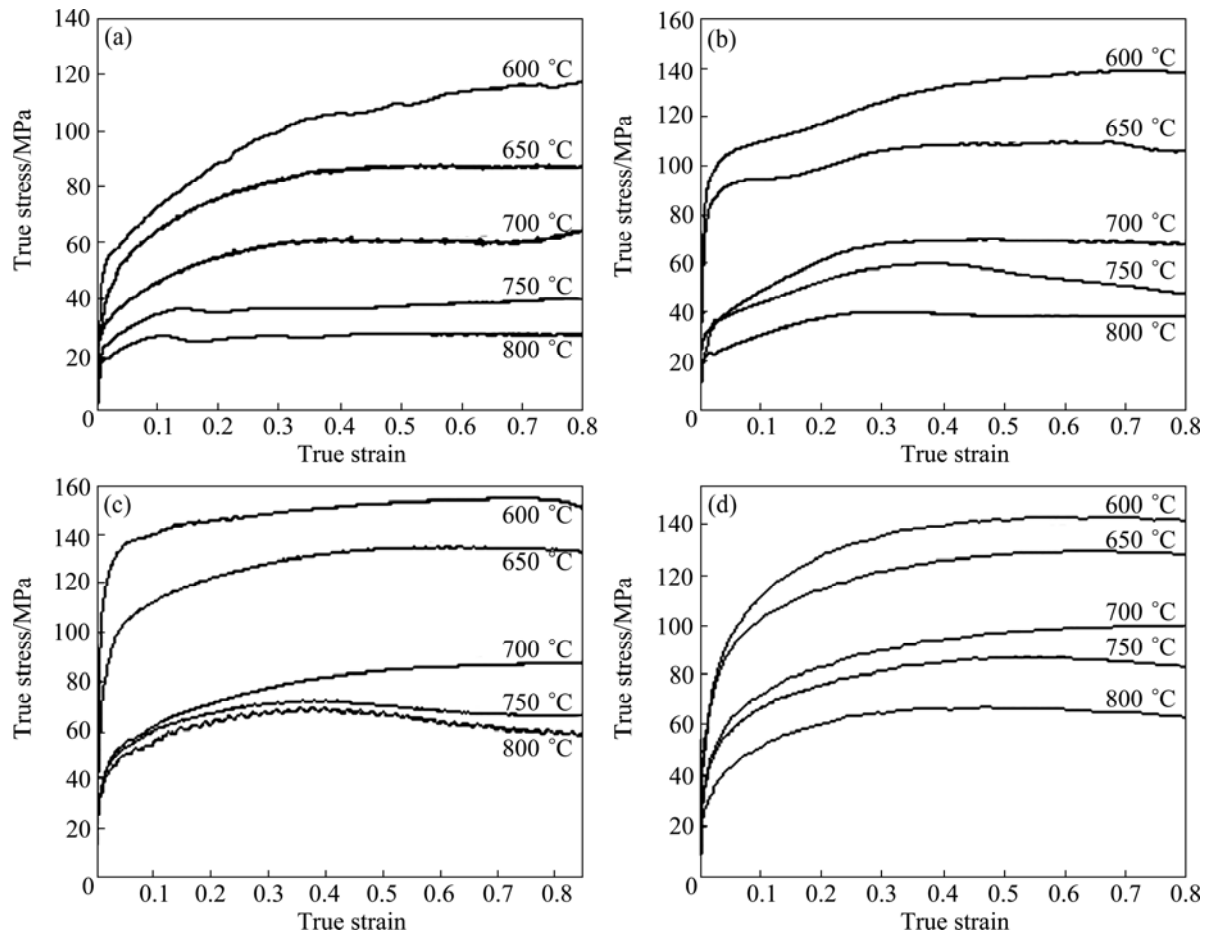


Fig. 2 True stress—true strain curves for Cu–Ni–Si–P alloy during hot compression deformation at various temperature and different strain rates: (a) $\dot{\varepsilon}=0.01 \text{ s}^{-1}$; (b) $\dot{\varepsilon}=0.1 \text{ s}^{-1}$; (c) $\dot{\varepsilon}=1 \text{ s}^{-1}$; (d) $\dot{\varepsilon}=5 \text{ s}^{-1}$

calculated value of α is 0.016. Figures 3(c) and (d) show the linear relationships between $\ln \dot{\varepsilon}$ and $\ln[\sinh(\alpha\sigma)]$, and between $\ln[\sinh(\alpha\sigma)]$ and T^{-1} , respectively. The calculated values of n and Q are 7.06 and 485.6 kJ/mol, respectively. The value of Q is higher than that of the polycrystalline copper with different purities (210 kJ/mol for 6N and 7N Cu, 245 kJ/mol for 4NCu) [14]. The higher deformation activation energy in hot deformation of Cu–8.0Ni–1.8Si–0.15Mg alloy (782.75 kJ/mol) was reported by ZHANG et al [6]. The increase of the activation energy for Cu–Ni–Si–P alloy is closely related to the change of the microstructural mechanism for hot deformation due to the precipitations of Ni_2Si and Ni_3P , which can play a role in extra obstacles for moving dislocations and hence increases the flow stress level during hot deformation.

Based on the experimental data and the results obtained above, the constitutive equation for Cu–Ni–Si–P alloy can be expressed as

$$\dot{\varepsilon} = 4.62 \times 10^{23} [\sinh(0.016\sigma)]^{7.06} \exp[-485.6 \times 10^3 / (RT)] \quad (4)$$

3.3 Processing map

The dynamic materials model is often used to construct the processing map to identify the deformation mechanism and to predict the deformation defect. Actually, a processing map is plotted based on the power dissipation map which represents the response of material to the applied strain rate at a constant temperature. The stress—strain (σ versus $\dot{\varepsilon}$) curve and the flow behavior of materials are strongly dependent on the strain rate and temperature. The general form of the flow behavior at constant strain and temperature can be expressed as [15–20]

$$\sigma = K \dot{\varepsilon}^m \quad (5)$$

where K and m are constants. m can be obtained as:

$$m = \frac{\partial \ln \sigma}{\partial \ln \dot{\varepsilon}} \quad (6)$$

According to the dynamic materials model, the workpiece imposed deformation is considered a nonlinear and dissipative power element. The total power P dissipated by plastic work consists of two parts that are

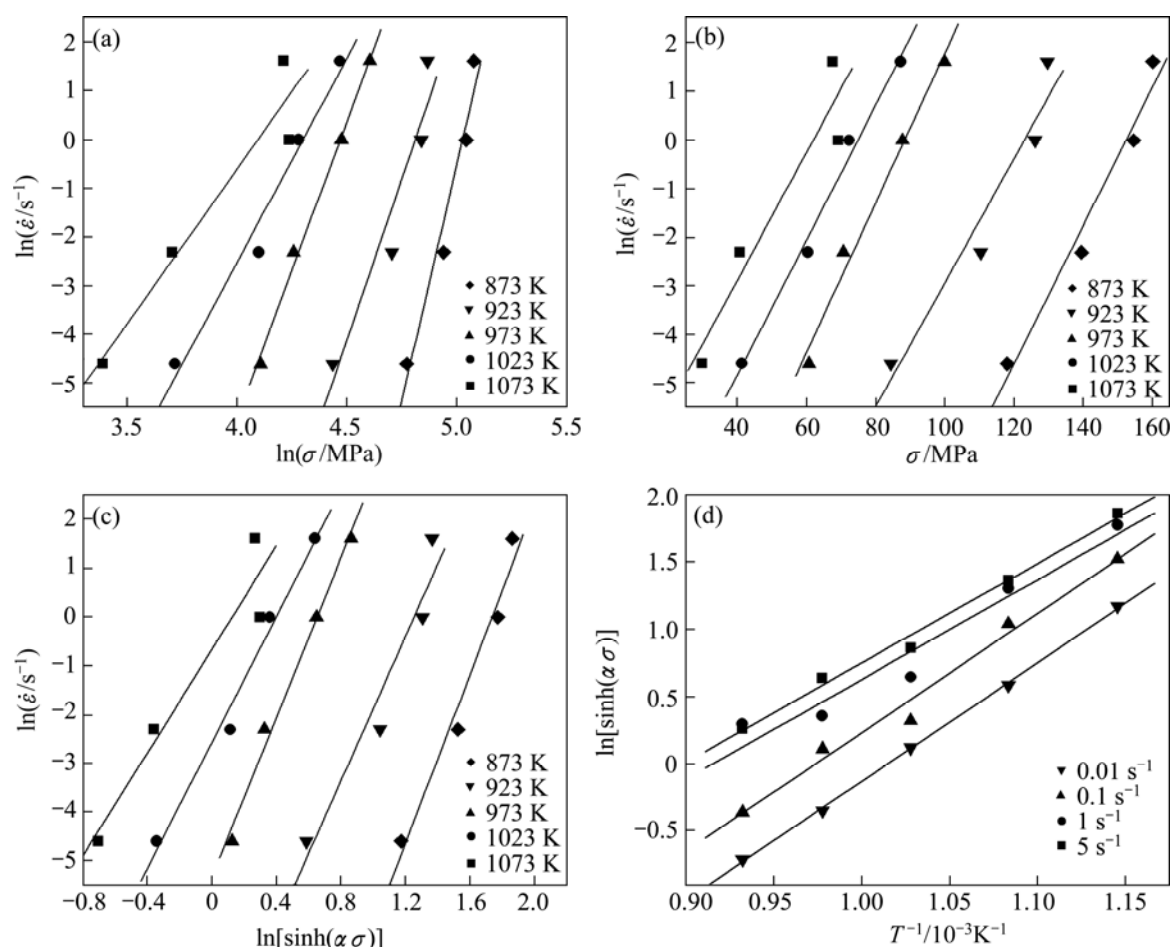


Fig. 3 Variations of peak stress (σ) with strain rate ($\dot{\epsilon}$) and deformation temperature (T) for Cu–Ni–Si–P alloy: (a) $\ln \sigma$ vs $\ln \dot{\epsilon}$; (b) σ vs $\ln \dot{\epsilon}$; (c) $\ln \dot{\epsilon}$ vs $\ln[\sinh(\alpha\sigma)]$; (d) T^{-1} vs $\ln[\sinh(\alpha\sigma)]$

given by the sum of two integrals as follows:

$$P = \sigma \dot{\epsilon} = G + J = \int_0^{\dot{\epsilon}} \sigma d\dot{\epsilon} + \int_0^{\sigma} \dot{\epsilon} d\sigma \quad (7)$$

where σ is the flow stress; $\dot{\epsilon}$ is the strain rate. The first integral is defined as G content and represents the main power input dissipated in the form of a temperature rise. The second integral is defined as J co-content and is related to the power dissipated by metallurgical processes.

The power partitioning between G and J is controlled by the flow behavior of metals and alloys and is decided by the strain rate sensitivity, m , as follows:

$$m = \frac{dJ}{dG} = \frac{\dot{\epsilon} d\sigma}{\sigma d\dot{\epsilon}} \cong \frac{d \ln \sigma}{d \ln \dot{\epsilon}} \quad (8)$$

The dissipator co-content J can be written as

$$J = \frac{m}{m+1} \sigma \dot{\epsilon} \quad (9)$$

For an ideal linear dissipator, $m=1$ and $J_{\max} = \sigma \dot{\epsilon} / 2$. By normalizing the instantaneous J with the maximum value, the efficiency of power dissipation η can be

defined as

$$\eta = \frac{J}{J_{\max}} = \frac{2m}{m+1} \quad (10)$$

The efficiency of power dissipation, η , is a dimensionless parameter to indicate the power dissipation by microstructure evolution, and the material deformed in the condition with high efficiency of power dissipation shows high workability. A continuum criterion for the occurrence of flow instability is obtained by utilizing the principle of the maximum rate of entropy production and given by

$$\xi(\dot{\epsilon}) = \frac{\partial \ln[m/(m+1)]}{\partial \ln \dot{\epsilon}} + m \leq 0 \quad (11)$$

where $\xi(\dot{\epsilon})$ is the instability parameter. The flow instabilities are predicted to occur when $\xi(\dot{\epsilon})$ becomes negative. The instability map is superimposed on the dissipation map to obtain a processing map, which exhibits characteristics of different mechanisms.

The processing maps for the Cu–Ni–Si–P alloy at strains of 0.3 and 0.5 are shown in Figs. 4(a) and (b), which represent the critical strain and steady strain,

respectively. The contours represent constant efficiency of power dissipation marked as percent and shaded areas represent the instability regions. The numbers against each contour representing efficiency of power dissipation characterize the rate of microstructure evolution in the hot working process. It can be seen from Fig. 4 that the stability domain occurs at a low strain rate ($\leq 0.1 \text{ s}^{-1}$) and a high temperature ($\geq 750 \text{ }^{\circ}\text{C}$) with a high efficiency of 31%–37%. When the strain rate is more than 1 s^{-1} at low temperature ($\leq 650 \text{ }^{\circ}\text{C}$), the deformation is located at instability domain which is shown in the form of shade in the figures. During practical application, it is necessary to keep away from this domain and corresponding processing parameters.

3.4 Microstructural mechanism

In processing maps, the deformation zones with different efficiency of power dissipation have their corresponding deformation mechanisms. To investigate the microscopic deformation mechanisms and to verify the reliability of process parameter configuration predicted by processing maps, the microstructures of the workpiece deformed under the specific process parameter configuration at a few typical deformation zones are characterized and analyzed.

Figure 5 shows the microstructures of Cu–Ni–Si–P alloy at different conditions. Through the processing map, the flow instability domain and safe deformation domain have been determined. In the flow instability domains,

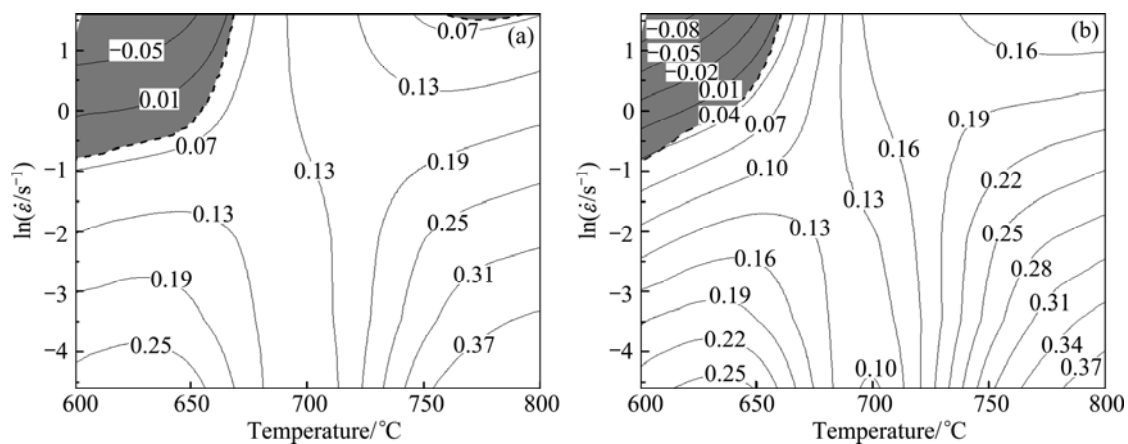


Fig. 4 Processing maps for Cu–Ni–Si–P alloy at different strains: (a) 0.3; (b) 0.5 (The numbers represent percent efficiency of power dissipation. Shaded domains represent the instability domains)

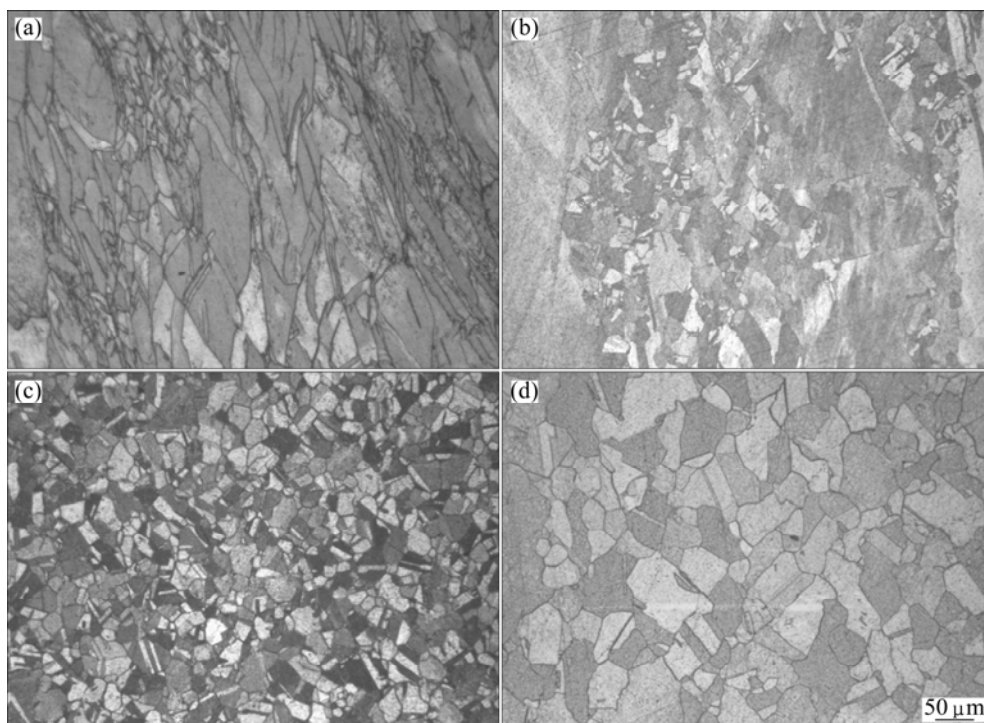


Fig. 5 SEM images of Cu–Ni–Si–P alloy hot deformed at different deformation conditions: (a) $600 \text{ }^{\circ}\text{C}$, 5 s^{-1} ; (b) $700 \text{ }^{\circ}\text{C}$, 0.1 s^{-1} ; (c) $750 \text{ }^{\circ}\text{C}$, 0.1 s^{-1} ; (d) $800 \text{ }^{\circ}\text{C}$, 0.01 s^{-1}

typical microstructural manifestations are adiabatic shear band formation, flow localization, dynamic strain aging, mechanical twinning and kinking or flow rotations. However, the microstructure mechanisms of the safe domains correspond to dynamic recrystallization, dynamic recovery and superplasticity. Figure 5(a) presents the microstructures under the deformation condition of (600 °C, 5 s⁻¹) and indicates that a large number of shear bands are obtained, which have typical characteristic of flow instability deformation. It also can be seen from Fig. 5 that the dynamic recrystallization takes place for the alloy deformed at high temperatures and low strain rates. The dynamic recrystallization zone obtained during testing at a temperature of 800 °C and strain rate of 0.01 s⁻¹ is shown in Fig. 5(d). These observations reveal that the strain rate range of 0.01–0.1 s⁻¹ is the dynamic recrystallization domain. It is safe for the Cu–Ni–Si–P alloy hot deformation processing. The optimum range for the Cu–Ni–Si–P alloy hot deformation processing in the safe domain obtained from the processing map is 750–800 °C at the strain rate of 0.01–0.1 s⁻¹. The alloy with this process has been successfully trial-produced by Chinalco Luoyang Copper Co., Ltd, China.

Based on these analyses and observations of the microstructure evolution at different deformation conditions, it is found that the process parameter configuration and optimization based on processing maps is a feasible approach for process parameter determination. These results can be used to design the hot-forging process of the good-quality product of the Cu–Ni–Si–P alloy.

4 Conclusions

1) The flow stress of the Cu–Ni–Si–P alloy increases with increasing strain rate and decreasing deformation temperature. It can be concluded that the dynamic recrystallization temperature of alloy is around 700 °C from the flow stress behavior of the Cu–Ni–Si–P alloy at various strain rates and deformation temperatures.

2) The dependence of flow stress on strain rate and temperature can be modeled by the constitutive exponential equation and the material constants are determined. The hot deformation activation energy for dynamic recrystallization is determined as 485.6 kJ/mol. The constitutive equation of the Cu–Ni–Si–P alloy can be expressed as

$$\dot{\varepsilon} = 4.62 \times 10^{23} [\sinh(0.016\sigma)]^{7.06} \exp[-485.6 \times 10^3 / (RT)]$$

3) The processing maps for the Cu–Ni–Si–P alloy obtained at strains of 0.3 and 0.5 predict the instability

regimes occurring at the strain rate more than 1 s⁻¹ and low temperature (≤ 650 °C). These temperatures and strain rates should be avoided in processing the alloy. The optimum processing condition is defined as low strain rate (≤ 0.1 s⁻¹) and high temperature (≥ 750 °C) with high efficiency of 31%–37%.

4) Through microstructure characterization and analysis, it is concluded that the Cu–Ni–Si–P alloy exhibits flow instability at higher strain rate and low temperature. The optimum range for the Cu–Ni–Si–P alloy hot deformation processing in the safe domain obtained from the processing map is 750–800 °C at the strain rate of 0.01–0.1 s⁻¹.

References

- [1] LEI J, LIN X, XIE H, LU Z L, WANG X. Abnormal improvement on electrical conductivity of Cu–Ni–Si alloys resulting from semi-solid isothermal treatment [J]. *Mater Lett*, 2012, 77: 107–109.
- [2] SUN W H, XU H H, LIU S H, DU Y, YUAN Z H, HUANG B Y. Phase equilibria of the Cu–Ni–Si system at 700 °C [J]. *J Alloys Compd*, 2011, 509: 9776–9781.
- [3] LONG Y Q, LIU P, LIU Y, ZHANG W M, PAN J S. Simulation of recrystallization grain growth during re-aging process in the Cu–Ni–Si alloy based on phase field model [J]. *Mater Lett*, 2008, 62: 3039–3042.
- [4] ZHAO D M, DONG Q M, LIU P. Structure and strength of the age hardened Cu–Ni–Si alloy [J]. *Materials Chemistry and Physics*, 2003, 79: 81–86.
- [5] LIU P, KANG B X, CAO X G. Aging precipitation and recrystallization of solidified Cu–Cr–Zr–Mg alloy [J]. *Mater Sci Eng A*, 1999, 265: 262–267.
- [6] ZHANG L, LI Z, LEI Q, QIU W T, LUO H T. Hot deformation behavior of Cu–8.0Ni–1.8Si–0.15Mg alloy [J]. *Mater Sci Eng A*, 2011, 528: 1641–1647.
- [7] NIEWCZAS M, EVANGELISTA E, BLAZ L. Strain localization during a hot compression test of Cu–Ni–Cr–Si–Mg alloy [J]. *Scripta Metallurgica et Materialia*, 1992, 27: 1735–1740.
- [8] ROBI P S, DIXIT U S. Application of neural networks in generating processing map for hot working [J]. *Journal of Materials Processing Technology*, 2003, 142: 289–294.
- [9] MOMENI A, DEGHANI K. Hot working behavior of 2205 austenite–ferrite duplex stainless steel characterized by constitutive equations and processing maps [J]. *Mater Sci Eng A*, 2011, 528: 1448–1454.
- [10] WANG K L, LU S Q, FU M W, LI X, DONG X G. Optimization of β /near- β forging process parameters of Ti–6.5Al–3.5Mo–1.5Zr–0.3Si by using processing maps [J]. *Materials Characterization*, 2009, 60: 492–498.
- [11] SELLARS C M, MCPEGART W J. On the mechanism of hot deformation [J]. *Acta Metal*, 1966, 14(9): 1136–1138.
- [12] ANBUSELVAN S, RAMANATHAN S. Hot deformation and processing maps of extruded ZE41A magnesium alloy [J]. *Mater Des*, 2010, 31: 2319–2323.
- [13] RAJAMUTHAMILSELVAN M, RAMANATHAN S. Hot deformation behaviour of 7075 alloy [J]. *J Alloys Compd*, 2011, 509: 948–952.
- [14] GAO W, BELYAKOV A. Dynamic recrystallization of copper polycrystals with different purities [J]. *Mater Sci Eng A*, 1999, 265: 233–238.

- [15] MORAKABATI M, ABOUTALEBI M, KHEIRANDISH S H, KARIMI TAHERI A, ABBASI S M. High temperature deformation and processing map of a NiTi intermetallic alloy [J]. *Intermetallics*, 2011, 19: 1399–1404.
- [16] SUN Y, ZENG W D, ZHAO Y Q, ZHANG X M, SHU Y, ZHOU Y G. Research on the hot deformation behavior of Ti40 alloy using processing map [J]. *Mater Sci Eng A*, 2011, 528: 1205–1211.
- [17] CHIB A, LEE S H, HIROAKI MATSUMOTO, MITSURU NAKAMURA. Construction of processing map for biomedical Co–28Cr–6Mo–0.16N alloy by studying its hot deformation behavior using compression tests [J]. *Mater Sci Eng A*, 2009, 513–514: 286–293.
- [18] RAO K P, PRASAD Y V R K, SURESH K. Hot working behavior and processing map of a c-TiAl alloy synthesized by powder metallurgy [J]. *Mater Des*, 2011, 32: 4874–4881.
- [19] ZHU Y C, ZENG W D, LIU J L, ZHAO Y Q, ZHOU Y G, YU H Q. Effect of processing parameters on the hot deformation behavior of as-cast TC21 titanium alloy [J]. *Mater Des*, 2012, 33: 264–272.
- [20] ZHANG H, ZHANG H G, PENG D H. Hot deformation behavior of KFC copper alloy during compression at elevated temperatures [J]. *Transactions of Nonferrous Metals Society of China*, 2006, 16: 562–566.

Cu–Ni–Si–P 合金热变形行为及热加工图

张 毅¹, 刘 平², 田保红¹, 刘 勇¹, 李瑞卿¹, 许倩倩¹

1. 河南科技大学 材料科学与工程学院, 洛阳 471003;
2. 上海理工大学 材料科学与工程学院, 上海 200093

摘 要: 采用高温等温压缩试验, 对 Cu–Ni–Si–P 合金在应变速率 $0.01\sim 5^{-1}$ 、变形温度 $600\sim 800\text{ }^{\circ}\text{C}$ 条件下的高温变形行为进行了研究, 得出了该合金热压缩变形时的热变形激活能 Q 和本构方程。根据实验数据与热加工工艺参数构建了该合金的热加工图, 利用热加工图对该合金在热变形过程中的热变形工艺参数进行了优化, 并利用热加工图分析了该合金的高温组织变化。热变形过程中 Cu–Ni–Si–P 合金的流变应力随着变形温度的升高而降低, 随着应变速率的提高而增大, 该合金的动态再结晶温度为 $700\text{ }^{\circ}\text{C}$ 。该合金热变形过程中的热变形激活能 Q 为 485.6 kJ/mol 。通过分析合金在应变为 0.3 和 0.5 时的热加工图得出该合金的安全加工区域的温度为 $750\sim 800\text{ }^{\circ}\text{C}$, 应变速率为 $0.01\sim 0.1\text{ s}^{-1}$ 。通过合金热变形过程中高温显微组织的观察, 其组织规律很好地符合热加工图所预测的组织规律。

关键词: Cu–Ni–Si–P 合金; 热压缩变形; 动态再结晶; 本构方程; 热加工图

(Edited by Hua YANG)